Biogeosciences, 21, 911–928, 2024
https://doi.org/10.5194/bg-21-911-2024

Biogeosciences Open Access EGU

Potential impacts of cable bacteria activity on hard-shelled benthic foraminifera: implications for their interpretation as bioindicators or paleoproxies

Maxime Daviray[1], Emmanuelle Geslin[1], Nils Risgaard-Petersen[2], Vincent V. Scholz[3], Marie Fouet[4], and Edouard Metzger[1]

[1]Univ Angers, Nantes Université, Le Mans Université, CNRS, Laboratoire de Planétologie et Géosciences, LPG UMR 6112, 49000 Angers, France
[2]Aquatic Biology, Department of Biology, Aarhus University, 8000 Aarhus C, Denmark
[3]Center for Electromicrobiology, Department of Biology, Aarhus University, 8000 Aarhus C, Denmark
[4]UMR CNRS 5805 EPOC – OASU, Station Marine d'Arcachon, Université de Bordeaux, CNRS, 33120 Arcachon, France

Correspondence: Maxime Daviray (maxime.daviray@univ-angers.fr)

Received: 19 September 2023 – Discussion started: 21 September 2023
Revised: 4 December 2023 – Accepted: 2 January 2024 – Published: 20 February 2024

Abstract. Hard-shelled foraminifera are protists able to build a calcareous or agglutinated shell (called a "test"). Here we study the impact of sediment acidification on calcareous test preservation. For this study, sediment cores were sampled in the macrotidal Auray estuary located on the French Atlantic coast. Living and dead foraminifera were quantified until 5 cm depth and discriminated using the Cell-Tracker™ Green vital marker. The pH and oxygen profiles combined with quantitative polymerase chain reaction (qPCR) suggested that cable bacteria were most likely to cause the acidifying process. Cable bacteria (CB) are filamentous bacteria coupling sulfide oxidation to oxygen reduction over centimetre distances, generating a strong pH gradient within the first few centimetres of the sediment that could affect the microhabitats occupied by benthic foraminifera. On two different intertidal mudflats, volumetric filament densities have been estimated. They were comparable to those observed in the literature for coastal environments, with 7.4 ± 0.4 and $74.4 \pm 5.0\,\mathrm{m\,cm^{-3}}$ per bulk sediment, respectively. Highly contrasting sediment acidification (from low to very intense) was described from 1.0 to 2.4 ΔpH. This seems to lead to various dissolution stages of the foraminiferal calcareous test from intact to fully dissolved tests revealing the organic lining. The dissolution scale is based on observations of living *Ammonia* spp. and *Haynesina germanica* specimens under a scanning electronic microscope. Furthermore, dead foraminiferal assemblages showed a strong calcareous test loss and an organic lining accumulation throughout depth under low pH, hampering the test preservation in deep sediment. These changes in both living and dead foraminiferal assemblages suggest that cable bacteria must be considered in ecological monitoring and historical studies using foraminifera as bioindicators and paleoenvironmental proxies.

1 Introduction

Benthic foraminifera are unicellular meiofaunal organisms. Most species can build a hard shell (called a test) that can be agglutinated (cemented grains), hyaline calcareous (calcium carbonate) and porcelaneous calcareous (calcium carbonate enriched in magnesium). Benthic foraminifera are very abundant in marine areas (Martin, 2000) including transitional environments (Alve and Murray, 1999; Debenay et al., 2006). These systems located between marine and continental areas (i.e. littoral and estuarine zones) are subjected to high variability of environmental factors (e.g. tide, freshwater flows, evaporation, development of seagrass meadows) over seasonal cycles. Then, benthic foraminifera are sub-

jected to strong variability of physical and geochemical parameters such as temperature, salinity or pH that they must tolerate. Despite such variability, benthic foraminifera assemblages have been used in transitional environments as bioindicators for biomonitoring the ecological state as well as chemical test composition and as paleoenvironmental proxies to understand past ecosystem functioning (Martin, 2000; Murray, 2006; Katz et al., 2010; Keul et al., 2017; Durand et al., 2018). However, species with a calcareous test can be affected by sediment acidification and carbonate undersaturation, leading to test dissolution (Le Cadre et al., 2003; Bentov et al., 2009; de Nooijer et al., 2009; Haynert et al., 2011, 2014; Kurtarkar et al., 2011; Charrieau et al., 2018b). Even if they are rarely observed in situ, few studies have reported signs of severe test dissolution in living assemblages (e.g. Alve and Nagy, 1986; Buzas-Stephens, 2005; Polovodova and Schonfeld, 2008; Haynert et al., 2012; Cesbron et al., 2016; Charrieau et al., 2018a; Schönfeld and Mendes, 2022). These authors attribute these dissolution observations to low pH and undersaturation of the carbonate system, which would be due to abiotic conditions (anthropogenic pollution, freshwater intrusions) or more rarely to biotic ones (degradation of plants). Under laboratory conditions, Le Cadre et al. (2003) have shown that test dissolution of living *Ammonia becarri* starts at pH 7.0 after 5 d and can recalcify in standard conditions after 8 d. Charrieau et al. (2018c) have shown that *Elphidium crispum* decalcified earlier than *Ammonia* sp. under seawater acidification (9 and 30 d, respectively, at pH $\sim$ 7.25). These authors also showed that test dissolution occurred even more prematurely in brackish waters (before 9 d at pH $\leq$ 7.53).

Sediment acidification may be linked to cable bacteria activity. Cable bacteria (CB) were discovered by Pfeffer and co-workers in 2012. They are sulfide-oxidising filamentous multicellular procaryotes from the Desulfobulbaceae family. They live in marine and freshwater sediments all around the world (Risgaard-Petersen et al., 2015; Burdorf et al., 2017a). They inhabit a zone several centimetres thick from the oxic surface to the deep sulfidic sediment. CB generate a vertical bioelectrical current by coupling the cathodic oxygen or nitrate reduction at the sediment surface to the anodic sulfide oxidation at depth (Nielsen et al., 2010; Pfeffer et al., 2012; Risgaard-Petersen et al., 2012; Marzocchi et al., 2014). CB activity (CBA) strongly affects sediment geochemistry and results in a clear geochemical fingerprint: an oxygen decrease in the surface sediments combined with a pH maximum in this oxic zone, followed by a strong acidification of the pore water in the suboxic zone (Nielsen et al., 2010; Risgaard-Petersen et al., 2012, 2014; Meysman et al., 2015). It leads to iron sulfide and carbonate dissolution from the suboxic zone (Risgaard-Petersen et al., 2012; Rao et al., 2016; van de Velde et al., 2016) and possibly the calcareous shell of benthic organisms.

Benthic foraminifera live mainly in the topmost sediment. Cable bacteria also develop on the few topmost centimetres of the sediment, which can therefore lead to an environmental overlap of the bacterial and foraminiferal communities. Richirt et al. (2022) hypothesised that CBA could induce the dissolution of calcareous tests within the sediment of Lake Grevelingen (Netherlands). In the present study, we assess the impact of cable bacteria activity on the foraminiferal test preservation in sediment, testing the hypothesis that cable bacteria activity is responsible for depleting the preservation of calcareous foraminifera in benthic assemblages. To achieve this, CBA was characterised by oxygen and pH microprofiling and CB density quantified by qPCR on intertidal mudflats of the Auray estuary (French Atlantic coast). Foraminiferal calcareous test dissolution stages were defined and quantified thanks to the analysis of SEM images. Then, we described living and dead foraminiferal assemblages to assess the calcareous test loss.

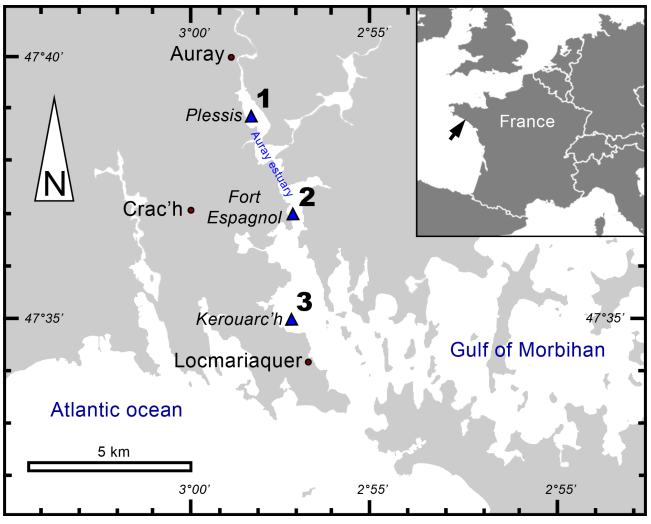

Figure 1. Locations of sampling stations in the intertidal mudflats of the Auray estuary (France).

2 Materials and methods

2.1 Studied area

The Gulf of Morbihan (Atlantic coast, France) is an enclosed marine bay where the Auray river flows. The Auray estuary is a macrotidal estuary with a tide range of about 4 m (Fig. 1).

Saltwater flows upstream over 20 km from the mouth of the estuary (357 m wide), which is tide-dominated (online data from OFB and IFREMER). The extensive description of this area (e.g. the marine influence, hydrodynamics and granulometry) has been reported by Fouet et al. (2022).

In September 2020, three stations along the Auray estuary were sampled on intertidal mudflats at low tide (Fig. 1 and Table 1): station 1 (Plessis), station 2 (Fort Espagnol) and station 3 (Kerouarc'h). Characteristics of the sampled stations are presented in Table 1.

Table 1. Characteristics of the stations sampled in September 2020. Temperature and salinity values correspond to these measured on the sampling day; weighted average and SD of sediment density data from a previous campaign in 2019. * Name of the station after Fouet et al. (2022).

Station	Coordinates	Distance from sea	T (°C)	Salinity	Sediment density ($g\,cm^{-3}$)	Vegetation cover
1 (*6B)	47.646° N, −2.972° W	12 km	24.4	29.6	1.71 ± 0.12	*Ulvea* mat
2 (*4B)	47.616° N, −2.953° W	8 km	21.2	38.5	1.67 ± 0.33	*Ulvea* mat
3 (*2C)	47.583° N, −2.955° W	4.3 km	21.5	34.3	1.51 ± 0.23	thick *Ulvea* mat few *Zostera*

2.2 Sediment sampling and processing

One core was sampled from each station by hand with a Plexiglas® tube (82 mm inner diameter, 50 mm depth) and was transported within an hour in a cool box to the field laboratory. Then, the cores were submerged in ambient seawater for at least 2 h to retrieve in situ conditions before microprofiling.

After microprofiling, each core was sliced using a core pusher and two trowels. Slice thickness was 2 mm for the first 20 mm depth and 10 mm up to 50 mm depth. Each sediment slice was treated with Cell-Tracker™ Green (CTG 5 CMFDA: 5-chloromethylfluorescein diacetate; Molecular Probes, Invitrogen Detection Technologies) to mark living benthic foraminifera by fluorescence (Bernhard et al., 2006; Bernhard and Bowser, 1996). A total of 1 mg of CTG was dissolved in 1 mL of dimethylsulfoxide (DMSO). This solution was then pipetted into the flask containing the sediment slice and its volume of ambient water to get a final solution of CTG about 1 µM (Bernhard et al., 2006; Cesbron et al., 2016; Langlet et al., 2013, 2014; Pucci et al., 2009). Each sample was then incubated in the dark at room temperature overnight and then fixed with 99 % ethanol (Choquel et al., 2021). Eventually, the samples were quickly and gently sieved with tap water over 315, 150, 125 and 63 µm mesh screens. Samples were conserved in 99 % ethanol.

DNA was extracted from subsamples of sediment slices at stations 1 and 2. A total of 1–2 g every second slice down to 18 mm depth was sampled with a heat-sterilised spatula and transferred to 2 mL Eppendorf tubes, then frozen at −20 °C. Samples were sent in dry ice ($CO_{2(s)}$ at −50 °C) to the Microbiology Institute of Biology in Aarhus University (Denmark) for qPCR analysis to quantify cable bacteria biomass.

2.3 Microsensor profiling

Two Unisense© profiling systems were used simultaneously. One consisted of two oxygen Clark-type microsensors with a 50 µm diameter tip (Revsbech and Jørgensen, 1986; Revsbech, 1989) and the other of a pH sensor with a 500 µm tip diameter (PH500, Unisense). They were both mounted on a motorised micromanipulator linked to a computer and connected to a MultiMeter WTW 3310. The increment was 50 µm until 3 mm for oxygen. It was 100 µm around the sediment–water interface (SWI) for pH, and it was adapted in real time according to the evolution of the observed profile until 50 mm depth. For each core, eight descents were managed for O_2 for a total of 16 profiles, while one profiling was done for pH. To calibrate the O_2 microsensor, two points were measured, with 100 % oxygen saturation in the bubbling seawater column and 0 % in the anoxic part of sediment. To calibrate the pH microsensor, three NBS buffers were used (values 4.0, 7.0, 9.2).

2.4 Living foraminiferal analyses

Counts of hard-shelled benthic foraminifera were performed in wet conditions (water) on the > 125 µm fractions using an epifluorescence stereomicroscope (Olympus SZX12 with a light source CoolLED pE-100, emission wavelength $\lambda = 470$ nm). All specimens showing clear green fluorescence were picked and identified. Remaining specimens were considered dead. In doubtful cases, particularly with agglutinated species, specimens were crushed to inspect whether fluorescence was due to the presence of protoplasm, the autofluorescence of sediment grains composing the test, or the presence of bacteria or nematodes living inside (Langlet et al., 2013; Cesbron et al., 2016). Total foraminiferal densities were expressed per 50 cm^2 of sediment and foraminiferal densities for sediment layers per 10 cm^3 volume.

For the taxonomy of hard-shelled foraminifera species, reference publications on estuarine foraminifera (Camacho et al., 2015; Richirt et al., 2019; Jorissen et al., 2023; Fouet et al., 2022; Feyling-Hanssen, 1972; Murray, 1979; Scott et al., 1980; Hayward et al., 2004; Hansen and Lykke-Andersen, 1976) and the World Register of Marine Species (2022) were used. The distinction between the *Ammonia* phylotypes (Richirt et al., 2019) being difficult, in particular on the dissolved tests, the results will be discussed at the genus level.

2.5 SEM imaging

Living foraminifera from three layers (0–2, 6–8, 40–50 mm depth), according to main pH features, were all observed under a scanning electronic microscope (SEM). Two different high-resolution SEMs were used: a DEBEN Hitachi TM4000 at the LPG (samples not metallised, 15 kV, wd = 6.5 mm, partial vacuum – 60 Pa) and a Zeiss EVO LS10 at the Service Commun d'Imageries et d'Analyses Microscopiques of Angers University (SCIAM; samples not metallised, 20 kV, wd = 6.5 mm, partial vacuum – 60 Pa, amperage 200 to 250 pA. Few scales of calcareous test dissolution of living foraminifera have been proposed in the literature (Corliss and Honjo, 1981; Le Cadre, 2003; Haynert et al., 2011; Gonzales et al., 2017; Charrieau et al., 2018a, 2022; Schönfeld and Mendes, 2022). These authors proposed scales varying from four to five different stages based on SEM images or stereomicroscope observations. They used a wide variety of morphological criteria to describe each dissolution stage (i.e. the number of calcite layers altered and chambers damaged, the presence of cracks or holes, whether the inner organic lining was visible, etc.). In the present study, we propose a scale of six dissolution stages based on SEM pictures of the two most abundant calcareous species in our living assemblages (*Ammonia* spp. and *Haynesina germanica*).

2.6 Dead foraminiferal analyses

Non-fluorescent tests of foraminifera were counted as dead specimens and picked in wet conditions (water) to preserve the organic linings from fully dissolved tests. We proceeded under a stereomicroscope (ZEISS Stemi sv11) in three sediment layers: the surface layer (0–2 mm), the subsurface layer (6–8 mm) and the deep layer (40–50 mm). After quick observations, when high densities were estimated (above 500 individuals; Patterson and Fishbein, 1989) fractions were split into eight subsamples using a wet splitter (Charrieau et al., 2018c).

2.7 Ratios in foraminiferal assemblages

In order to characterise the loss of calcareous specimens in the assemblages, we defined a ratio enabling each sample to be compared as follows.

$$C/T = \text{calcareous foraminifera/total foraminifera} \quad (1)$$

Calcareous foraminifera are counted regardless of their dissolution stage and total foraminifera include agglutinated individuals. To estimate the intensity of dissolution in the assemblage, we calculated the following ratio.

$$\text{DS-5}/C = \text{calcareous test at dissolution stage 5/ total calcareous foraminifera} \quad (2)$$

These ratios were calculated on both living and dead assemblages for layers 0–2 and 6–8 as well as 40–50 mm.

2.8 Statistical procedure

The putative relationship between cable bacteria activity and the advanced dissolution stages of the living calcareous test foraminifera was assessed by applying the parametric Fisher's test followed by the pair-wise Fisher's test for post hoc comparisons. To minimise the risk of type 1 error p values were FDR-adjusted. The significance level was set to 5 %. As the last layer of calcite produced during the growth of the foraminifera covers the entire test and is thinner than the others (Haynes, 1981; Hansen, 1999; Debenay et al., 2000; Boudagher-Fadel, 2018), DS-1 and DS-2 are more commonly observed, resulting from a process of gradual dissolution or precipitation of calcite. Discrimination of the effect of the dissolution process is therefore made on the alteration of several calcite layers as for DS-3 and above. For this purpose, the dissolution stages were combined into two groups: no to slight dissolution (DS-0, DS-1 and DS-2) and moderate to severe dissolution (DS-3, DS-4 and DS-5). These two groups were then compared between each of the three stations and between the different depth levels (0–2, 6–8, 40–50 mm depth) for each station. Statistics were calculated with R software using the "stats" and "rstatix" packages (R Core Team, 2022; Kassamaba, 2022).

2.9 Sediment treatment for DNA extraction and quantification

DNA was extracted from weighed amounts of sediment (0.22–0.25 g wet weight). DNA extraction was carried out using a DNeasy PowerLyzer PowerSoil Kit (Qiagen) and the DNA was collected in 60 µL elution buffer. The analysis followed the procedures outlined in Geelhoed et al. (2020). The primer combination of ELF645wF and CB836wR was used to target the 16S rRNA gene of the marine cable bacteria of the genus *Candidatus* Electrothrix Trojan, 2016. The calibration curves were obtained using a synthetic standard (sequence accession KR912339.1, position 611–912, synthesised by Eurofins Genomics, Denmark) diluted in a 10-fold dilution series. The standards and samples were run in triplicate. Each reaction contained the master mix (RealQ Plus 2× Master Mix Green, Low ROXTM, Ampliqon, Denmark), forward and reverse primers (0.2 µM), and BSA (1 µM). The qPCR was performed with a real-time PCR analyser (AriaMX, Agilent). The thermal cycles were as follows: 15 min at 95 °C for initial denaturation followed by 40 cycles of 15 s at 95 °C (denaturation), 30 s at 60 °C (annealing) and 20 s at 72 °C (amplification). Afterwards, the melting curve was obtained by 30 s at 95 °C, 30 s at 60 °C and 30 s at 95 °C. Finally, the temperature was held for 5 min at 40 °C to terminate the analysis. The results are reported as the unit gene copies(g wet sediment)$^{-1}$. CB filament density was calculated as in Geelhoed et al. (2020) using data on wet sediment density from a previous campaign in 2019 (Table 1) and expressed in m cm^{-3}. For administrative reasons, it was only

Table 2. Description of the six dissolution stages of the calcareous tests of *Ammonia* spp. and *Haynesina germanica*.

Dissolution stage	Name	SEM observations and stage descriptions	Figures
DS-0	Intact test	intact, glassy test with a smooth surface and cylindrical pores, no sign of dissolution	Figs. 3-1, 4-1
DS-1	Slight surface dissolved test	transparent test with cylindrical pores, alteration of the last calcite layer only, appearance of the interpore sutures in *H. germanica* (scarce in *Ammonia* spp., alteration more visible on the inter-chamber walls)	Figs. 3-2, 4-2
DS-2	Peeled test	dull, whitish test with some fusion of adjacent widen pores, calcite layers cracking and crumbling, last chamber often lost, thinner and blunt tubercular ornamentation of *H. germanica*	Figs. 3-3, 4-3
DS-3	Cracked test	opaque and cracked test with a strong alteration of all calcite layers, brittle test with holes, fusion of widen pores, the organic lining can be visible, loss of last chamber, broken ornamentation of *H. germanica*	Figs. 3-4, 4-4
DS-4	"Star-shaped" test	nearly completely dissolved test, only the inter-chamber walls remaining, the last chambers often absent, dissolved peripheral chambers with the inner organic lining visible	Figs. 3-5, 4-5
DS-5	Fully dissolved test	totally dissolved test revealing the inner organic lining, may keep the foraminifera shape allowing the identification of the genus *Ammonia* (not observed for *H. germanica*)	Fig. 3-6

possible to carry out these DNA analyses for stations 1 and 2.

3 Results

3.1 Microsensor profiles and cable bacteria abundance

Oxygen penetration depth in the sediment at stations 1, 2 and 3 was 1.4 ± 0.2, 0.9 ± 0.3 and 0.9 ± 0.2 mm, respectively. At station 1, pH rapidly decreased from 7.7 at the sediment–water interface (SWI) to a minimum of 6.8 at 15 mm depth. Below this minimum, pH stabilised to 7.2 around 40 mm depth. In contrast, at stations 2 and 3, pH increased immediately below the SWI from 7.8 to 8.1 at 0.8 mm depth and to 7.95 at 0.6 mm, respectively (Fig. 4). Below these maxima, pH reached a minimum of 5.8 at 7 mm depth at station 2 and of 6.3 between 7 and 19 mm depth at station 3. Below these minima, pH stabilised at 6.8 after 25 mm depth at station 2 and at 6.9 after 34 mm depth at station 3.

At station 1, the number of 16S CB copies of *Candidatus* Electrothrix ranged from $0.23 \pm 0.01 \times 10^7$ to $0.48 \pm 0.01 \times 10^7$ 16S copies(g wet sediment)$^{-1}$ and remained constant through depth (Fig. 4). At station 2, it amounted to $2.8 \pm 0.12 \times 10^7$ 16S copies(g wet sediment)$^{-1}$ in the upper 5 mm of sediment and progressively decreased to about $0.3 \pm 0.01 \times 10^7$ 16S copies(g wet sediment)$^{-1}$ in the 16–18 mm depth layer. The maximum 16S CB copies of *Ca.* Electrothrix at station 2 corresponded to the maximum pH in depth. According to Geelhoed et al. (2020) and using wet sediment density from the same stations obtained in 2019 (Marie Fouet, personal communication, 2022), we calculated a filament density of 7.4 ± 0.4 and 74.4 ± 5.0 m cm^{-3} at stations 1 and 2, respectively.

3.2 Hard-shelled benthic foraminiferal

3.2.1 Living foraminiferal diversities and densities

The foraminiferal species assemblages were typical of estuarine environments (Debenay et al., 2000), with a poor species richness (14, 13 and 18 species at stations 1, 2 and 3, respectively). *Ammonia* spp. and *Haynesina germanica* (Ehrenberg, 1840) both strongly dominated the assemblages at all three stations (25.1 % and 51.5 %, respectively, of the total assemblage for station 1, 14.5 % and 48.2 % for station 2, 7.3 % and 61.4 % for station 3; Fig. 5). *Ammonia* spp. included the species *Ammonia veneta* (Schultze, 1854) (phylotype T1 after Hayward et al., 2004), *Ammonia aberdoveyensis* Haynes, 1973 (phylotype T2 after Hayward et al., 2004) and *Ammonia confertitesta* Zheng, 1978 (phylotype T6 after Hayward et al., 2004). Agglutinated foraminifera represent 19.9 %, 25.7 % and 12.7 % of the total assemblage at stations

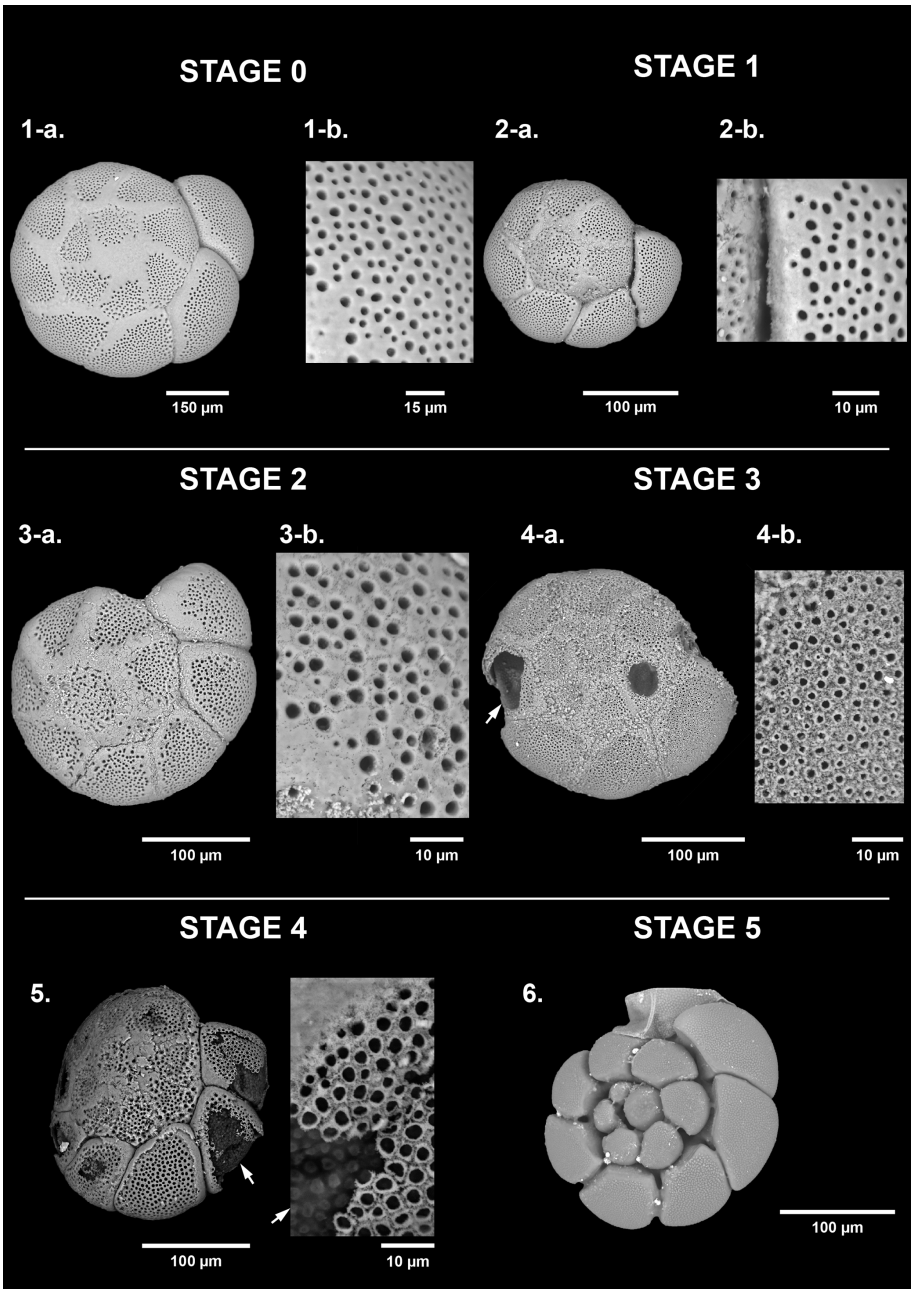

Figure 2. Dissolution scale of *Ammonia* spp. based on high-resolution SEM images (spiral view). The specimens are classified into six stages of test dissolution from intact (stage 0) to fully dissolved (stage 5). For stages 0 to 2, a zoom on the last formed chamber was done (**1**b, **2**b, **3**b) and on the *n*-1 chamber for stage 3 (**4**b). White arrows point to the organic lining.

1, 2 and 3, respectively. They were dominated by *Ammobaculites agglutinans* (d'Orbigny, 1846).

3.2.2 Living foraminiferal vertical distribution

Total densities of CTG-labelled foraminifera in cores 1, 2 and 3 were 1273, 548, and 1431 ind. 50 cm^{-2}, respectively. The highest densities were found in the first layer of sediment (0–2 mm depth) for all cores with 295, 137 and 371 ind. 10 cm^{-3} at stations 1, 2 and 3, respectively (Fig. 5), where dioxygen was available and pH was maximal (Fig. 4).

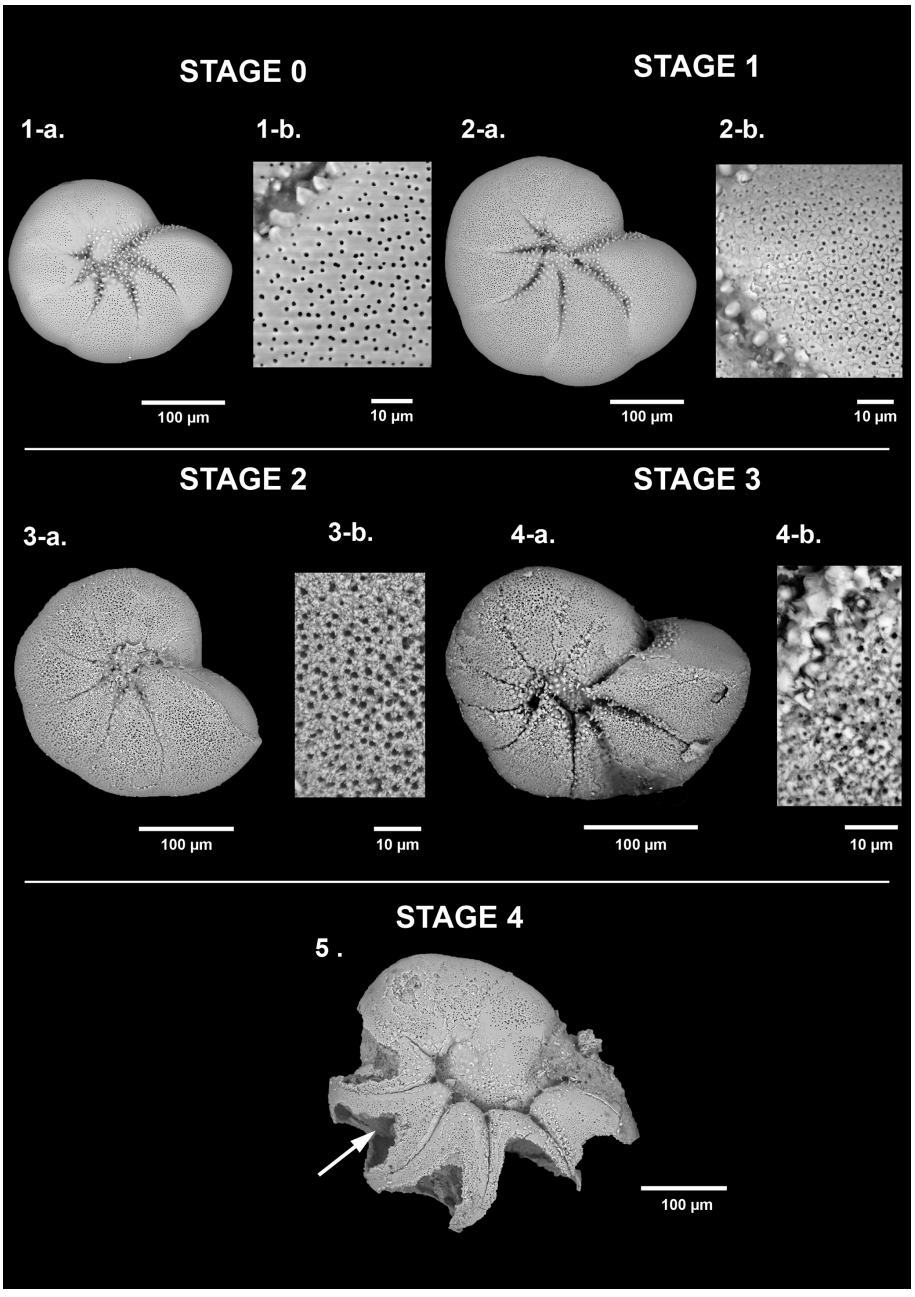

Figure 3. Dissolution scale of *Haynesina germanica* based on high-resolution SEM images. The specimens are classified into five stages of test dissolution from intact (stage 0) to the "star shape" (stage 4). No organic lining (stage 5) has been identified as belonging to the taxa *Haynesina*. For stages 0 and 1, a zoom on the last formed chamber was done (**1**b, **2**b) and on the n-1 chamber for stages 2 and 3 (**3**b, **4**b). The white arrow points to the organic lining.

At station 1, total density dropped below 2 mm to stabilise at 30 ± 9 ind. $10\,cm^{-3}$ (Fig. 5). At station 2, the vertical distribution of total densities showed two maxima: the first at the SWI and a second at 18–20 mm depth with 47 ind. $10\,cm^{-3}$. A first minimum of 11 ind. $10\,cm^{-3}$ was observed at 8–10 mm depth close to the lowest pH layer, and a second minimum of 5 ind. $10\,cm^{-3}$ was observed at the bottom of the core. At station 3, after a maximum at the SWI, foraminifera density decreased gradually with depth, following the pH trend, to reach on average 19 ± 4 ind. $10\,cm^{-3}$ from 20 to 50 mm depth.

At station 1, the ratio of calcareous foraminifera in the living foraminiferal assemblage (C/T) was 0.91 for the SWI (Table 3) and around 0.77 ± 0.07 for the layers below. At station 2, C/T was 0.97 of the SWI and on average 0.64 ± 0.16 between 2 and 50 mm depth (Appendix). However, agglu-

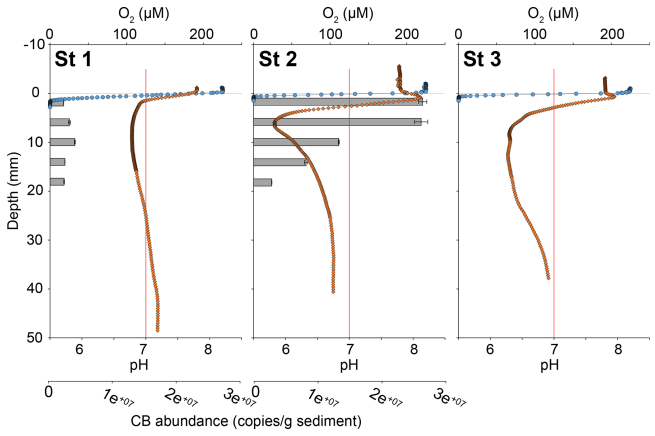

Figure 4. Sediment oxygen (blue circles) and pH (orange diamonds) microprofiles at the three stations and vertical distribution of cable bacteria abundance (qPCR of Ca. Electrothrix 16S rRNA gene copies, grey bars) for stations 1 and 2. 0 is the position of the sediment–water interface (SWI). The vertical red line represents neutral pH. The oxygen profile presented is one of those obtained by microprofiling and is representative of O_2 penetration for each station.

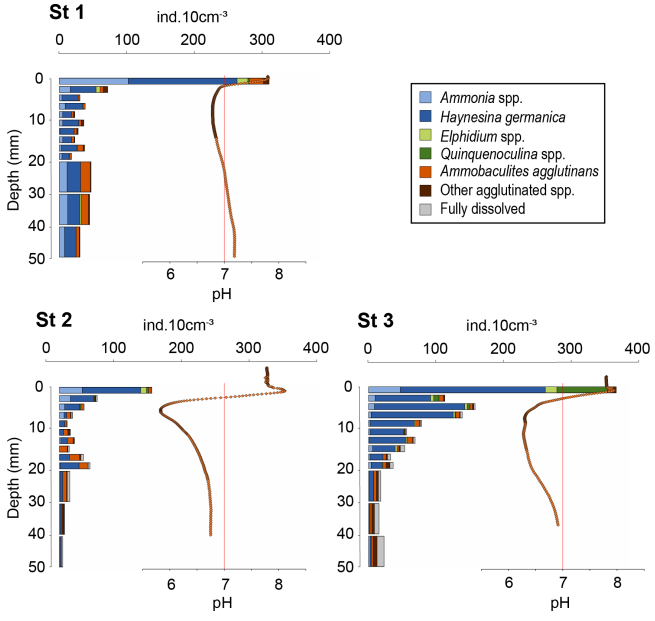

Figure 5. Vertical distributions of living foraminifera densities per $10\,cm^3$ of sediment at the three stations (> 125 µm fraction). 0 is the position of the sediment–water interface (SWI). Recall of pH microprofiles (orange diamonds) and neutral pH (vertical red line).

tinated taxa dominated the assemblages from 10 to 18 mm, just below the pH minimum, with a drop of C/T ratio to 0.39 ± 0.18 (Appendix). At station 3, the C/T ratio was 0.97 at the SWI and decreased asymptotically as calcareous foraminiferal densities vanished to reach 0.72 ± 0.15 below 20 mm after the pH minimum zone (Appendix).

3.2.3 Calcareous test dissolution of living foraminifera

Figure 6 shows the dissolution stage (DS) of calcareous foraminifera for three selected sediment layers (0–2, 6–8, 40–50 mm) for living assemblages. At station 1, living specimens with a calcareous test showed low alteration. The DS remained stable through depth ($p > 0.05$). Specimens with "intact tests" (DS-0) or "slight surface dissolved tests" (DS-1) represented 90 % of calcareous foraminifera. The strongest dissolution stages were DS-2 ("peeled test") and DS-3 ("cracked test"), accounting for less than 10 %.

Conversely, at station 2, many foraminifera were very fragile under manipulation. Numerous "fully dissolved tests" (DS 5) with only the organic lining were observed through depth ($50\,ind.\,50\,cm^{-2}$; Appendix). At the SWI (0–2 mm layer), DS-0 and DS-1 tests represented 95 % of the calcareous test foraminifera in the living assemblage. Only a few DS-2 and DS-5 specimens were present. In the subsurface level (6–8 mm depth), corresponding to the most acidic conditions, no DS-0 and DS-1 specimen was observed. DS-4 and DS-5 tests were about 40 % of the calcareous tests observed. At the deepest layer (40–50 mm), DS-5 specimens were dominant (> 50 %). The surface layer was significantly different ($p < 0.005$) from the two deeper layers that showed no significant differences ($p = 0.267$).

At station 3, many foraminifera were fragile under manipulation, and DS-5 specimens were abundant through depth with about $140\,ind.\,50\,cm^{-2}$ (Appendix). At the SWI (0–2 mm layer) and in the subsurface level (6–8 mm depth), DS-0 and DS-1 specimens represented about 75 %, while DS-2 accounted for 20 %. Few specimens of DS-3, DS-4 and DS-5 were observed. At the deepest layer (40–50 mm), DS-5 specimens were the most abundant calcareous test foraminifera (78 %). The severe DS groups (DS-3, DS-4 and DS-5) were significantly more overrepresented in the deep layer than in the surface and subsurface layers ($p < 0.005$). DS groups were not significantly different between the surface and subsurface ($p = 1$).

Overall, the exact Fisher's test revealed significant difference dissolution stages among stations ($p < 0.005$). The pairwise Fisher's exact test showed that the low DS groups (DS-0, DS-1, DS-2) were significantly overrepresented at station 1 compared to the two other stations ($p < 0.005$). Furthermore, there were no significant difference between stations 2 and 3 ($p = 0.532$).

3.2.4 Calcareous vs. agglutinated foraminifera in the dead assemblages

Species in the benthic foraminiferal thanatocoenosis were the same as in the living assemblages. At station 1, calcareous taxa dominated agglutinated ones in the dead assemblage with C/T ratios varying from 0.74 to 0.89 (Table 3). The proportion of organic lining (DS-5 / C) increased slightly with depth from 0.06 to 0.18. On the other hand, at station 2, ag-

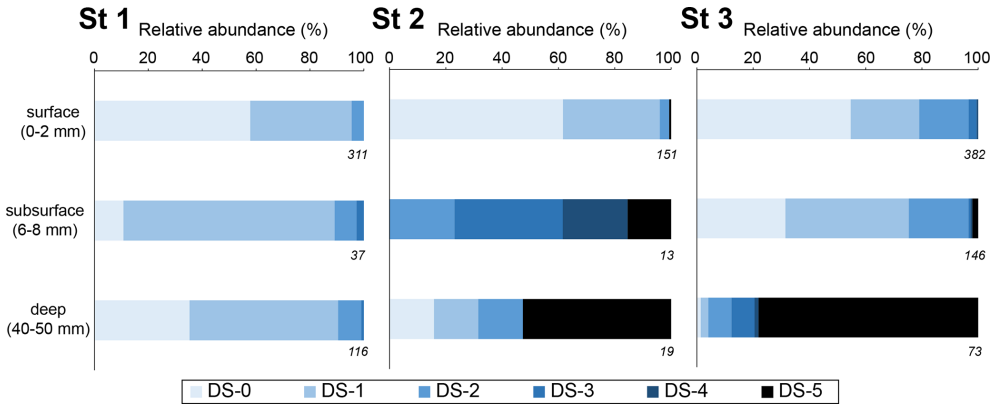

Figure 6. Relative abundance of living benthic foraminifera with a calcareous test for each dissolution stage for 10 cm^3 of sediment (*Ammonia* spp. and *H. germanica* from the > 125 µm fraction). Three depth levels were analysed: the surface (0–2 mm; oxic zone), the subsurface (6–8 mm; suboxic zone corresponding to pH minimum) and the deeper (40–50 mm; anoxic zone). The numbers on the lower right of the boxes are the total numbers of SEM-photographed specimens.

glutinated taxa dominated the dead assemblage in the surface and subsurface levels (C/T ratio of 0.43 and 0.36, respectively) but not in the deepest one even if they remained abundant (0.65; Table 3). The DS-5 / C ratio was very high in all three depth layers, remaining > 0.70. At station 3, the C/T ratio remained high in the dead assemblage of both the surface and subsurface with 0.88 and 0.83, and it decreased strongly to 0.36 in depth where agglutinated specimens were dominant. The DS-5 / C ratio increased with depth, from 0.06 at the surface to 0.95 in the deeper layer.

Comparing dead and living assemblages, it can be noted that for station 1, C/T ratios were not very different whatever the depth (Table 3). Stations 2 and 3 showed much lower C/T ratios in the dead assemblages, indicating a marked loss of calcareous foraminifera during taphonomic processes, although this difference is not significant. In addition, stations 2 and 3 showed a higher occurrence of DS-5 tests in the dead assemblages, resulting in high DS-5 / C ratios. In detail, station 2 showed the highest DS-5 / C ratio in the subsurface layer (0.96) where pH is minimal, while station 3 showed a strong increase in this ratio in the deepest layer (0.95).

4 Discussion

4.1 Is cable bacteria activity responsible for pore water acidification in the mudflats of the Auray estuary?

Oxygen and pH microprofiles recorded at stations 2 and 3 showed the typical fingerprint of cable bacteria activity (CBA): a pH maximum within the oxic zone without oxygen production followed by a significant acidification into the suboxic zone (Fig. 4; Nielsen et al., 2010; Pfeffer et al., 2012; Risgaard-Petersen et al., 2012; Meysman et al., 2015). The presence of cable bacteria within the upper first centimetre at station 2 was further confirmed by the qPCR data. The calculated filament density of about 70 m cm^{-3} at this station was of the same order of magnitude as the in situ densities reported from the Baltic Sea (Marzocchi et al., 2018; Hermans et al., 2019), bivalve reefs (Malkin et al., 2017), subtidal mudflats (van de Velde et al., 2016) and intertidal salt marshes (Larsen et al., 2015). The geochemical signature at station 1 is less clear regarding CBA although the qPCR data indicated CB filament density in the low range of the in situ densities reported from the Baltic Sea (Marzocchi et al., 2018; Hermans et al., 2019). Here, there was no pH peak in the oxic zone and the suboxic acidification was the weakest compared to stations 2 and 3 ($\Delta pH < 1.0$ and ΔpH of 2.3 and 1.6, respectively). As the sediment acidification continued at least 5 mm below the oxic zone (oxygen penetration depth < 2 mm depth) for the three stations, oxic processes such as pyrite oxidation are unlikely to explain such pH decrease. However, the anaerobic oxidation of reduced compounds such as manganese, iron or sulfide could be involved in the pore water acidification (Soetaert et al., 2007; Middelburg et al., 2020) but the observed acidification was too high to be explained by such processes (van Cappellen and Wang, 1996; Soetaert et al., 2007). Therefore, we suggest that acidification was mainly driven by cable bacteria activity rather than any other geochemical process.

The diversity of pH microprofiles observed between the three stations could indicate a contrasting intensity of the cable bacteria activity between stations. According to the low filament abundance and the low range of pH ($\Delta pH = 1.0$) at station 1, CBA would be minimal and it would have a limited impact on the sediment geochemistry. Conversely, the strong abundance and pH range ($\Delta pH = 2.4$) suggest the most intense cable bacteria activity at station 2, whereas the pH range ($\Delta pH = 1.8$) at station 3 suggests an intermediate to high CBA. It is possible that such variability from one mudflat to another can be explained by the stage of development of the bacterial community and/or by the specific geochem-

Table 3. Densities of living and dead foraminifera for each depth layer at the three all stations (ind. $10\,cm^{-3}$ of sediment). Depth correspondences: surface (0–2 mm), subsurface (6–8 mm) and deep (4–5 mm). The "calcareous" class includes the DS-5 specimens (fully dissolved test showing the organic lining). A: agglutinated, C: calcareous; the ratios are those described in the "Materials and methods" section.

		Living foraminifera					Dead foraminifera				
		Agglutinated (A)	Calcareous (C)	Fully dissolved test (DS-5)	C/T ratio	DS-5 / C ratio	Agglutinated (A)	Calcareous (C)	Fully dissolved test (DS-5)	C/T ratio	DS-5 / C ratio
St 1	surface (0–2 mm)	30	295	0	0.91	0.00	212	589	38	0.74	0.06
	subsurface (6–8 mm)	3	36	0	0.92	0.00	21	153	22	0.88	0.14
	deep (40–50 mm)	6	26	0	0.81	0.00	94	772	141	0.89	0.18
St 2	surface (0–2 mm)	4	137	1	0.97	0.01	373	282	197	0.43	0.70
	subsurface (6–8 mm)	7	12	2	0.63	0.17	181	104	100	0.36	0.96
	deep (40–50 mm)	1	4	2	0.80	0.50	239	453	327	0.65	0.72
St 3	surface (0–2 mm)	12	371	0	0.97	0.00	58	418	49	0.88	0.12
	subsurface (6–8 mm)	7	137	3	0.95	0.02	45	214	53	0.83	0.25
	deep (40–50 mm)	9	14	11	0.61	0.79	493	274	259	0.36	0.95

ical composition of each mudflat from upstream to downstream (Malkin et al., 2014, 2017; Rao et al., 2016). Our observations suggest that *Ulvea* mats observed at stations 2 and 3 during core sampling in autumn (Table 1) could play a role in CB development. Several studies showed that macrophyte decay is rather slow compared to microphytobenthic mineralisation and favours free-sulfide production and upward diffusion (Anschutz et al., 2007; Metzger et al., 2007; Cesbron et al., 2014; Delgard et al., 2016), which are favourable conditions for CB development. Previous observations confirm the spatial and seasonal cable bacteria activity dynamics (e.g. Seitaj et al., 2015; Lipsewers et al., 2017; Malkin et al., 2022; Hermans et al., 2019). Most publications refer to a boom-and-bust cycle of CB in laboratory incubations and to the seasonal alternation of the sulfur-oxidising bacterial community in the field as a function of hypoxia events inducing seasonal pH variability. However, no desoxygenation or strong and recursive reworking events have been reported in the presently studied area during the previous weeks before sampling, which is reoxygenated at each low tide (Fouet, 2022; OFB and IFREMER data). Each low tide could lead to the reactivation of cable bacteria activity in these highly eutrophic mudflats. The most intense resuspension phenomenon here would be rising tide (Menier and Dubois, 2011; Menier et al., 2011) or bioturbation. The benthic macrofauna (> 2 mm) of the mudflats is dominated by polychaetes of *Nephtys* spp. known to burrow into the sediments (Michaud et al., 2021; abundance around 8 ind. $50\,cm^{-2}$, Oihana Latchere, personal communication, 2023). The variability between the stations could be the result of bioturbation modulating acidification within the subsurface sediment layer (Malkin et al., 2014, 2017, 2022; Aller et al., 2019). Unfortunately, there is little literature on cable bacteria activity under a tidal cycle. Currently, the control factors of spatial and temporal discrepancies of the cable bacteria density and the CBA are still unresolved and need more investigations.

The cable bacteria activity causes pH anomalies that impact sediment geochemistry and lead to the carbonate dissolution process as described in Risgaard-Petersen et al. (2012), Meysman et al. (2015), Rao et al. (2016), van de Velde et al. (2016) and Malkin et al. (2017). It has been supposed that this dissolution process could be responsible for foraminiferal test dissolution (Risgaard-Petersen et al., 2012; Richirt et al., 2022). Considering the increase in observations of cable bacteria activity occurrence in a wide range of coastal and marine environments (Burdorf et al., 2017; Scholz et al., 2021), we assume that the potential impact of this bacterial acidification of sediment on carbonate meiofauna should be strongly considered.

4.2 Impacts of sediment acidification on living foraminifera

We show in Figs. 4 and 6 that advanced dissolution stages 3, 4 and 5 were significantly overrepresented at stations 2 and 3, where acidification was important, compared to station 1 where no DS-5 was observed. More precisely, vertical DS distribution corresponded to vertical acidity variability at stations 2 ($0.01 < \text{DS-5} / C < 0.50$) and 3 ($0.00 < \text{DS-5} / C < 0.79$). There was no indication for such depth distribution at station 1 where pH variability was the lowest ($\text{DS-5} / C = 0$). The relative abundance of calcareous specimens over agglutinated (C/T) was very stable along depth at station 1 (0.78 ± 0.07; Appendix), whereas this ratio was more variable at stations 2 and 3 (0.65 ± 0.17 and 0.73 ± 0.15, respectively), confirming that pH conditions affected the assemblage composition through the underrepresentation of calcareous foraminifera (Fig. 5) . Species diversity appeared not to be affected because most of the foraminiferal population lived in the thin oxic zone, which is not affected by the strong pH decrease. Our data suggest that the sediment acidification on the mudflats, supposedly due to cable bacteria activity, has a drastic effect on the integrity of living benthic foraminiferal tests and potentially on their assemblages. The magnitude of this effect may depend on the dissolution process intensity and duration throughout the life cycle of foraminifera.

Since the dataset of the present study is rather limited, one can examine literature data that provide oxygen and pH microprofiles with the sub-centimetre vertical distribution of living foraminifera in intertidal mudflats and other benthic environments. Geochemical data from an intertidal mudflat of the Arcachon basin in the French Atlantic coast suggest sediment acidification in May 2011 at station N (Cesbron et al., 2016) with a $\Delta pH = 1.6$ and a pH minimum of 6.2 well below the oxic zone at 20 mm depth. At the same station in July 2011, all calcareous benthic foraminifera specimens showed a fully dissolved test with the organic lining remaining (DS-5 / $C = 1$). The assemblage also showed that *Eggerella scabra*, an agglutinated species, strongly dominated the foraminiferal assemblage at all depths down to 50 mm, except for the 0 to 5 mm layer ($C/T = 0.88 \pm 0.02$ for the uppermost layer; $C/T = 0$ below). The authors assumed that test dissolution resulted from a strong acidification of the sediments due to an intense remineralisation of the relict roots of *Zostera*. We can assume here that these roots provided the refractory material that enhanced sulfate reduction (Anschutz et al., 2007; Metzger et al., 2007; Cesbron et al., 2014; Delgard et al., 2016), providing enough free sulfide to favour cable bacteria development that could drive the dissolution process as probably happened at stations 2 and 3 of the Auray estuary in the present study. However, Cesbron and co-workers also showed that during winter (February 2011), foraminifera showed less dissolution due to a lower intensity of diagenetic processes including free-sulfide production and probably benthic acidification. These results underline the importance of the temporal variability of diagenetic processes that influence pore water geochemistry and eventually calcareous test integrity. They also question the time integration of pH conditions recorded in the foraminifera tests as foraminifera may have mechanisms to buffer pH variations as suggested by different studies (de Nooijer et al., 2009b, 2014; Toyofuku et al., 2017) or vertical migration strategies (Geslin et al., 2004; Pucci et al., 2009; Koho et al., 2011; Hess et al., 2013). It could be assumed that the dissolution of the calcareous foraminifera tests would respond to integrated dynamics over a few days to a few weeks (Le Cadre, 2003; Charrieau et al., 2018b, 2022). These microorganisms are capable of recalcifying their test following acidification events with the same daily to weekly dynamics (Le Cadre et al., 2003). This dynamic is relatively comparable to the oxidation processes of the reduced mineral phases that can generate acidification of the sediment, as is cable bacteria activity. We therefore assume that the tests of dead specimens incorporate the variability of these dynamics to a greater or lesser extent. These dynamics should be investigated in the future in the Auray estuary to better understand differences of dissolution stages observed between stations. It can also be assumed that tolerance to acidification may be species-dependent. Under laboratory experiments, Charrieau et al. (2018a) have shown that *Ammonia* sp. specimens survived longer than *Elphidium crispum* under the same conditions of salinity, pH and Ω_{calc} (20–34, 7.3–7.9 and 0.4–2.7, respectively). Mojtahid et al. (2023) have observed that low DIC ($< 900\,\mu mol\,kg^{-1}$) affected growth and survival of *Bulimina marginata* and *Cassidulina laevigata* but not *Ammonia confestitesta*, while a pH and Ω_{calc} decrease did not affect any of the three species (other parameters constant, $pH > 7.5$, $\Omega_{calc} \geq 1$). McIntyre-Wressnig et al. (2014) have seen no effect of acidification on *Bolivina argentea* and *Bulimina marginata* ($S \sim 34$, $TA \sim 2400\,\mu mol\,kg^{-1}$, $pH \geq 7.5$). Furthermore, Haynert et al. (2011) have shown that *Ammonia aomoriensis* slightly decalcified as soon as $pH \sim 7.7$ and $\Omega_{calc} > 1$ and showed severe dissolution at $pH \leq 7.4$ and $\Omega_{calc} < 1$. However, the same species cultured in their natural sediment was unaffected in the same geochemical conditions (Haynert et al., 2014). It suggests that sediment chemistry provides a microhabitat to support benthic foraminiferal community growth and development even under sediment acidification. These interesting results have emphasised the complex and misunderstood interaction between calcareous test foraminifera and the carbonate system that needs more detailed investigations.

Conversely, a tidal mudflat from another estuarine system of the French Atlantic coast seems not to show indices of the acidification process or occurrence of dissolution on living foraminifera. Living foraminifera from the Brillantes mudflat of the Loire estuary were studied at two stations in September 2012 and April 2013 (Thibault de Chanvalon et al., 2015, 2022). The vertical distribution of living foraminifera reported in the Loire mudflat was similar to the vertical distribution of station 2 reported in the present study with a maximal density at the topmost layer within the oxic zone, a minimal density around 10 mm depth and a second maximum below. However, no foraminiferal test dissolution was reported by Thibault de Chanvalon and co-workers and the foraminiferal assemblages were heavily dominated by calcareous foraminiferal species, resulting in a DS-5 / C ratio equal to zero and a C/T ratio of about 1. Furthermore, at these stations, pH profiles did not show strong acidification or a CBA fingerprint on different occasions (May 2013, February 2014, June 2018, unpublished data). The pH decrease corresponded to oxygen uptake and was below 0.5 units with a minimum of about 7.7. No pH peak at the interface was observed in a profile performed in the dark. The major difference between these systems is the size of the river that induces significant resuspension–deposition events for the Loire estuary (network SYVEL, GIP Loire Estuaire). In addition, bioturbation seems to be intense at the Brillantes mudflat (Thibault de Chanvalon et al., 2015, 2016b, 2017). Another difference between these studies is the absence of macrophytes at the studied stations of the Brillantes mudflat. Finally the size of the catchment area of the Loire provides an important flux of suspended particles rich in metallic oxides that will, once settled in the mudflat, generate a thick layer of sediment where the iron cycle dominates diagenetic processes acting as an efficient "iron curtain" that maintains free

sulfide between 5 and 10 cm depth (Thibault de Chanvalon et al., 2016a, b). These combined conditions are not favourable to cable bacteria development (Malkin et al., 2014, 2017). Foraminiferal observations strongly suggest the absence of a dissolution process in the studied part of the Brillantes mudflat. This area may be considered a control station.

Other studies reporting calcareous test dissolution of benthic living foraminifera in transitional environments are published but without geochemical data, allowing discussion of potential causes of the dissolution process (Alve and Nagy, 1986; Buzas-Stephens, 2005; Polovodova and Schonfeld, 2008; Bentov et al., 2009; de Nooijer et al., 2009; Kurtarkar et al., 2011; Haynert et al., 2012; Schönfeld and Mendes, 2022). Although the hypotheses put forward by these authors on the causes of test dissolution are all plausible (environmental pollution, freshwater inputs, organic matter degradation), they are not strongly explained. Therefore, the absence of pH data (Buzas-Stephens, 2005; Polovodova and Schonfeld, 2008) or their insufficient vertical resolution (Alve and Nagy, 1986; Haynert et al., 2012; Schönfeld and Mendes, 2022) does not exclude the potential involvement of cable bacteria in those environments. In the Baltic Sea, which could be considered a sort of giant estuary, Charrieau et al. (2018a) provide pH microprofiles that seem to indicate the absence of strong acidification (all sites combined: minimum pH 7.17; maximum ΔpH 0.6). However, these authors observed calcareous test dissolution of living foraminifera and concluded that dissolution may be the consequence of a complex set of environmental factors whose ecological equilibrium can change rapidly in such coastal areas (salinity, oxygen concentration, pH and Ω_{calc}). Laboratory experiments conducted by these authors (Charrieau et al., 2018b) seem to indicate that low salinity may be an important factor for calcareous test dissolution. The difference from estuarine studies discussed above is probably that salinity change dynamics in the Baltic are rather minor compared to salinity in the Auray and Loire that are macrotidal systems with species adapted to such salinity variations.

4.3 Impacts of sediment acidification on dead assemblages and shell preservation

Richirt et al. (2022) have assumed that calcium carbonate undersaturation in the suboxic zone resulting from cable bacteria activity could be responsible for low densities of calcareous tests in the dead assemblages recorded in sediments of Lake Grevelingen. Our results suggest that acidification, as CBA could induce, strongly affects the calcareous test integrity and the assemblage composition of living foraminifera before taphonomic processes. Our study also suggests that after foraminifera death, dissolution processes keep transforming the foraminifera assemblage during test burial, supporting the hypothesis formulated by Richirt et al. (2022). Comparing C/T and DS-5 / C ratios between living and dead assemblages at different depths, we relate in detail the impact of pH distribution on taphonomic loss. Under low acidification (like at station 1), calcareous tests were relatively well preserved. At this station, the community structure between living and dead assemblages varied slightly (C/T ranged from 0.81 to 0.98 in the living assemblage and from 0.74 to 0.89 in the dead assemblage). The occurrence of dissolution in the living assemblage was zero, while in the dead assemblage the DS-5 / C ratio increased with depth from 0.06 to 0.18, indicating that the low dissolution generated a relatively slow taphonomic process. Calcareous tests dominated both living and dead assemblages with an increase in this trend with depth in the dead assemblage confirming the good preservation of calcareous foraminifera. Where sediment acidification was moderate (like at station 3), the dissolution effect on the thanatocoenosis was gradual with depth. Calcareous test density decreased through the wide acidic layer (C/T decrease from above 0.8 to 0.36 at 50 mm depth) and there was an accumulation of fully dissolved tests showing only their organic linings in dead foraminiferal assemblages at depth (DS-5 / C of 0.95). This feature suggests that the moderate dissolution generated a gradual taphonomic process leading to a noticeable calcareous loss with depth. Eventually, under a strong and intense dissolution process (like at station 2), the effect occurred mostly within the restricted acidic layer. The calcareous tests disappeared from the dead foraminiferal assemblage in this subsurface layer, while the fully dissolved tests showing only their organic linings and agglutinated tests accumulated ($C/T = 0.37$ and DS-5 / $C = 0.96$). At depth, the dead foraminiferal assemblage showed fairly high densities that are comparable to stations where acidification was less intense. As the living specimens were quite rare, such accumulation of dead tests suggested that somehow they bypassed the acidic firewall of the suboxic layer. If tests arrived at depth through sedimentary burial the acidic firewall was possibly variable through time and not constantly established. If sediment acidification is more constant, physical or biological reworking buried them sufficiently fast to preserve tests from corrosive conditions and mechanic crumbling. Here, regardless of the alkalinity or calcium carbonate content of the sediment, if living and dead calcareous foraminifera are decalcified so intensely, the corrosive conditions are intense enough over time to generate dissolution in organisms, which alive can fight off these hostile conditions to a greater or lesser extent, as they are somehow adapted to the strong physical and biogeochemical dynamics of transitional environments.

At this stage, these hypotheses cannot be assessed. One can note the high concentration of dead fully dissolved tests in the first 2 mm (0.70) where pH is the most alkaline, suggesting that sedimentary reworking may have brought dead specimens from the subsurface acidic layer to the surface. Further studies on dead assemblages are needed to statistically validate the CBA vs. calcareous test loss relationship.

With low pH and carbonate undersaturation in pore water, the dissolution process resulting from cable bacteria activ-

ity could leave an imprint on taphonomy and on historical records yet to be explored. Indeed, it may alter the carbonate composition of the remaining calcareous tests used as geochemical proxies based on isotopic fractioning or trace elements (Katz et al., 2010; Petersen et al., 2018; Mojtahid et al., 2023).

In this case, CBA may be considered a potential factor in the seasonal perturbation of sediment geochemistry in interpretations of foraminiferal assemblages of historical studies. As proposed in Richirt et al. (2022), historical records of benthic foraminifera could be used to reconstruct past CBA and determine the age of the first cable bacteria occurrence in the studied environments. A multivariate approach coupling the identification of lipid biomarkers in cable bacteria or eDNA, the study of foraminiferal species assemblages (C/T ratio), test preservation and isotopic test composition, and the characterisation of the paleoenvironment by sedimentology and sediment geochemistry could allow us to distinguish the bacterial activity from other factors responsible for test dissolution. Therefore, associating it with major environmental changes through time, light could be shed on the original factors of this bacterial spreading discovered only 10 years ago: have they always been present without us having the tools to detect them, or have they appeared recently and are spreading around the world?

5 Conclusions

This original study suggests that sediment acidification caused by cable bacteria activity could be responsible for significant calcareous test foraminifera dissolution patterns. As a result, proportions of calcareous test would change in both living and dead assemblages. The proportion of fully dissolved tests showing only their organic linings would increase in the living assemblages in the suboxic and anoxic zones of the sediment, as well as in the thanatocoenosis. In order to better understand this cause-and-effect relationship and reduce the uncertainty factors raised here, further in situ studies would need to be carried out in further locations over different periods, especially including the carbonate system. Laboratory incubation experiments would also provide a better understanding of the potential impact of this bacterial activity on the resilience of foraminiferal communities. It should allow us to learn more about the integration of their response in the historic record. Based on these hypotheses, we ask what implications they might have for environmental interpretations of data from foraminifera used as paleoproxies or bioindicators. Eventually, we could be able to provide a historical retrospective on the presence of cable bacteria in marine sediments and their impact on the carbonate system and benthic meiofauna.

Appendix A

Table A1. Foraminiferal absolute densities and ratios in the Auray estuary for the three stations.

	Depth layer	Layer volume (cm^{-3})	*Haynesina germanica*	*Ammonia* spp.	*Elphidium* spp.	*Quinqueloculina* spp.	DS-5 specimen	*Ammobaculites agglutinans*	Other agglutinans	Total	*C* / *T* ratio	DS-5 / *C* ratio
	0–2 mm	10.6	179	113	18	2	0	23	9	344	0.91	0.00
	2–4 mm	10.6	42	18	6	0	0	5	7	78	0.85	0.00
	4–6 mm	10.6	26	4	0	0	0	3	0	33	0.91	0.00
	6–8 mm	10.6	28	9	1	0	0	3	0	41	0.93	0.00
	8–10 mm	10.6	15	5	0	0	0	3	2	25	0.80	0.00
	10–12 mm	10.6	26	5	0	0	0	4	4	39	0.79	0.00
St 1	12–14 mm	10.6	23	1	0	0	0	4	2	30	0.80	0.00
	14–16 mm	10.6	15	5	0	0	0	4	1	25	0.80	0.00
	16–18 mm	10.6	25	3	1	0	0	9	2	40	0.73	0.00
	18–20 mm	10.6	12	4	1	0	0	3	0	20	0.85	0.00
	20–30 mm	52.8	110	61	2	0	0	77	6	256	0.68	0.00
	30–40 mm	52.8	99	67	11	0	2	57	9	245	0.73	0.01
	40–50 mm	52.8	93	42	2	0	0	28	4	169	0.81	0.00
	0–2 mm	10.6	95	37	9	3	1	4	0	149	0.97	0.01
	2–4 mm	10.6	38	18	1	0	2	1	1	61	0.97	0.03
	4–6 mm	10.6	24	8	2	0	0	5	0	39	0.87	0.00
	6–8 mm	10.6	4	7	0	0	2	6	1	20	0.65	0.15
	8–10 mm	10.6	8	0	0	0	1	3	0	12	0.75	0.11
	10–12 mm	10.6	6	0	0	0	1	7	3	17	0.41	0.14
St 2	12–14 mm	10.6	11	2	0	0	0	10	2	25	0.52	0.00
	14–16 mm	10.6	0	0	0	0	2	13	1	16	0.13	1.00
	16–18 mm	10.6	16	0	0	0	4	17	2	39	0.51	0.20
	18–20 mm	10.6	31	1	0	0	3	15	0	50	0.70	0.09
	20–30 mm	52.8	22	6	2	0	20	33	6	89	0.56	0.40
	30–40 mm	52.8	15	5	0	0	4	5	8	37	0.65	0.17
	40–50 mm	52.8	9	0	0	0	10	5	1	25	0.76	0.53
	0–2 mm	10.6	238	52	19	83	0	8	5	405	0.97	0.00
	2–4 mm	10.6	91	11	5	8	0	7	2	124	0.93	0.00
	4–6 mm	10.6	148	9	4	4	2	4	2	173	0.97	0.01
	6–8 mm	10.6	133	4	3	1	3	6	1	151	0.95	0.02
	8–10 mm	10.6	73	2	2	0	2	6	1	86	0.92	0.03
	10–12 mm	10.6	55	2	1	0	2	1	1	62	0.97	0.03
St 3	12–14 mm	10.6	60	1	2	0	3	8	1	75	0.88	0.05
	14–16 mm	10.6	37	6	3	0	7	3	2	58	0.91	0.13
	16–18 mm	10.6	21	2	0	0	5	5	2	35	0.80	0.18
	18–20 mm	10.6	18	4	1	0	5	5	6	39	0.72	0.18
	20–30 mm	52.8	38	4	0	0	21	20	16	99	0.64	0.33
	30–40 mm	52.8	7	4	1	0	35	15	19	81	0.58	0.74
	40–50 mm	52.8	8	9	1	0	57	15	32	122	0.61	0.76

Data availability. All of the data are published within this paper and in the Supplement. The raw data used to make the figures are available on request.

Author contributions. MD: foraminiferal and geochemical analysis, writing, review and editing. EG: head of CB for the CNRS project, foraminiferal analysis, writing, review and editing. NRP: statistical inference, writing, review and editing. VVS: qPCR proceeding, review and editing. MF: fieldwork, review and editing. EM: microprofile acquisition, writing, review and editing.

Competing interests. At least one of the (co-)authors is a member of the editorial board of *Biogeosciences*. The peer-review process was guided by an independent editor, and the authors also have no other competing interests to declare.

Disclaimer. Publisher's note: Copernicus Publications remains neutral with regard to jurisdictional claims made in the text, published maps, institutional affiliations, or any other geographical representation in this paper. While Copernicus Publications makes every effort to include appropriate place names, the final responsibility lies with the authors.

Acknowledgements. The authors are grateful to Sophie Quinchard for assistance with the foraminifera picking, Sophie Sanchez for sample splitting (LPG, Université d'Angers) and Romain Mallet (SCIAM, Université d'Angers) for the achievement of part of the SEM imaging. Susanne Nielsen and Ian Marshall (Aarhus University) are thanked for assistance with the qPCR analysis. The authors are grateful to Frans Jorissen for fieldwork and his advice for the writing process (LPG, Université d'Angers). The authors thank the participants in the field trips (2019 and 2020). The authors also

thank Sebastiaan van de Velde, Sairah Malkin and the three anonymous reviewers for their constructive comments. The authors thank Jack Middelburg for his work as an editor.

Financial support. This research has been supported by the Centre National de la Recherche Scientifique (LEFE-CYBER CB-For) and the Office Français de la Biodiversité (FORESTAT, grant no. 3976-CT-RD-AMI-18-SURV-FORESTAT).

Review statement. This paper was edited by Jack Middelburg and reviewed by Sebastiaan van de Velde, Sairah Malkin, and one anonymous referee.

References

Aller, R. C., Aller, J. Y., Zhu, Q., Heilbrun, C., Klingensmith, I., and Kaushik, A.: Worm tubes as conduits for the electrogenic microbial grid in marine sediments, Sci. Ad., 5, eaaw3651, https://doi.org/10.1126/sciadv.aaw3651, 2019.

Alve, E. and Murray, J. W.: Marginal marine environments of the Skagerrak and Kattegat: a baseline study of living (stained) benthic foraminiferal ecology, Palaeogeogr. Palaeocl., 146, 171–193, https://doi.org/10.1016/S0031-0182(98)00131-X, 1999.

Alve, E. and Nagy, J.: Estuarine foraminiferal distribution in Sandebukta, a branch of the Oslo Fjord (Norway), J. Foramin. Res., 16, 261–284, https://doi.org/10.2113/gsjfr.16.4.261, 1986.

Anschutz, P., Chaillou, G., and Lecroart, P.: Phosphorus diagenesis in sediment of the Thau Lagoon, Estuar. Coast. Shelf Sci., 72, 447–456, https://doi.org/10.1016/j.ecss.2006.11.012, 2007.

Bentov, S., Brownlee, C., and Erez, J.: The role of seawater endocytosis in the biomineralization process in calcareous foraminifera, P. Natl. Acad. Sci. USA, 106, 21500–21504, https://doi.org/10.1073/pnas.0906636106, 2009.

Bernhard, J. M. and Bowser, S. S.: Novel epifluorescence microscopy method to determine life position of foraminifera in sediments, J. Micropalaeontol., 15, 68–68, https://doi.org/10.1144/jm.15.1.68, 1996.

Bernhard, J. M., Ostermann, D. R., Williams, D. S., and Blanks, J. K.: Comparison of two methods to identify live benthic foraminifera: A test between Rose Bengal and CellTracker Green with implications for stable isotope paleoreconstructions: Foraminifera Viability Method Comparison, Paleoceanography, 21, PA4210, https://doi.org/10.1029/2006PA001290, 2006.

Boudagher-Fadel, M. K.: Biology and Evolutionary History of Larger Benthic Foraminifera, in: Evolution and Geological Significance of Larger Benthic Foraminifera, UCL Press, 1–44, https://doi.org/10.2307/j.ctvqhsq3.3, 2018.

Burdorf, L. D. W., Tramper, A., Seitaj, D., Meire, L., Hidalgo-Martinez, S., Zetsche, E.-M., Boschker, H. T. S., and Meysman, F. J. R.: Long-distance electron transport occurs globally in marine sediments, Biogeosciences, 14, 683–701, https://doi.org/10.5194/bg-14-683-2017, 2017a.

Burdorf, L. D. W., Tramper, A., Seitaj, D., Meire, L., Hidalgo-Martinez, S., Zetsche, E.-M., Boschker, H. T. S., and Meysman, F. J. R.: Long-distance electron transport occurs globally in marine sediments, Biogeosciences, 14, 683–701, https://doi.org/10.5194/bg-14-683-2017, 2017b.

Buzas-Stephens, P.: Population Dynamics and Dissolution of Foraminifera in Nueces Bay, Texas, J. Foramin. Res., 35, 248–258, https://doi.org/10.2113/35.3.248, 2005.

Camacho, S. G., Moura, D. M. de J., Connor, S., Scott, D. B., and Boski, T.: Taxonomy, ecology and biogeographical trends of dominant benthic foraminifera species from an Atlantic-Mediterranean estuary (the Guadiana, southeast Portugal), Palaeontol. Electron., 18, 1–27, https://doi.org/10.26879/512, 2015.

Cesbron, F., Metzger, E., Launeau, P., Deflandre, B., Delgard, M.-L., Thibault de Chanvalon, A., Geslin, E., Anschutz, P., and Jézéquel, D.: Simultaneous 2D Imaging of Dissolved Iron and Reactive Phosphorus in Sediment Porewaters by Thin-Film and Hyperspectral Methods, Environ. Sci. Technol., 48, 2816–2826, https://doi.org/10.1021/es404724r, 2014.

Cesbron, F., Geslin, E., Jorissen, F. J., Delgard, M. L., Charrieau, L., Deflandre, B., Jézéquel, D., Anschutz, P., and Metzger, E.: Vertical distribution and respiration rates of benthic foraminifera: Contribution to aerobic remineralization in intertidal mudflats covered by *Zostera noltei* meadows, Estuar. Coast. Shelf Sci., 179, 23–38, https://doi.org/10.1016/j.ecss.2015.12.005, 2016.

Charrieau, L. M., Filipsson, H. L., Nagai, Y., Kawada, S., Ljung, K., Kritzberg, E., and Toyofuku, T.: Decalcification and survival of benthic foraminifera under the combined impacts of varying pH and salinity, Mar. Environ. Res., 138, 36–45, https://doi.org/10.1016/j.marenvres.2018.03.015, 2018a.

Charrieau, L. M., Filipsson, H. L., Nagai, Y., Kawada, S., Ljung, K., Kritzberg, E., and Toyofuku, T.: Decalcification and survival of benthic foraminifera under the combined impacts of varying pH and salinity, Mar. Environ. Res., 138, 36–45, https://doi.org/10.1016/j.marenvres.2018.03.015, 2018b.

Charrieau, L. M., Bryngemark, L., Hansson, I., and Filipsson, H. L.: Improved wet splitter for micropalaeontological analysis, and assessment of uncertainty using data from splitters, J. Micropalaeontol., 37, 191–194, https://doi.org/10.5194/jm-37-191-2018, 2018c.

Charrieau, L. M., Nagai, Y., Kimoto, K., Dissard, D., Below, B., Fujita, K., and Toyofuku, T.: The coral reef-dwelling *Peneroplis* spp. shows calcification recovery to ocean acidification conditions, Sci. Rep., 12, 6373, https://doi.org/10.1038/s41598-022-10375-w, 2022.

Choquel, C., Geslin, E., Metzger, E., Filipsson, H. L., Risgaard-Petersen, N., Launeau, P., Giraud, M., Jauffrais, T., Jesus, B., and Mouret, A.: Denitrification by benthic foraminifera and their contribution to N-loss from a fjord environment, Biogeosciences, 18, 327–341, https://doi.org/10.5194/bg-18-327-2021, 2021.

Corliss, B. H. and Honjo, S.: Dissolution of Deep-Sea Benthonic Foraminifera, Micropaleontology, 27, 356–378, https://doi.org/10.2307/1485191, 1981.

Debenay, J.-P., Guillou, J.-J., Geslin, E., and Lesourd, M.: Crystallization of Calcite in Foraminiferal Tests, Micropaleontology, 46, 87–94, 2000.

Debenay, J.-P., Bicchi, E., Goubert, E., and Armynot du Châtelet, E.: Spatio-temporal distribution of benthic foraminifera in relation to estuarine dynamics (Vie estuary, Vendée, W France), Estuar. Coast. Shelf Sci., 67, 181–197, https://doi.org/10.1016/j.ecss.2005.11.014, 2006.

Delgard, M. L., Deflandre, B., Kochoni, E., Avaro, J., Cesbron, F., Bichon, S., Poirier, D., and Anschutz, P.: Biogeochemistry of dissolved inorganic carbon and nutrients in seagrass (Zostera noltei) sediments at high and low biomass, Estuar. Coast. Shelf Sci., 179, 12–22, https://doi.org/10.1016/j.ecss.2016.01.012, 2016.

de Nooijer, L. J., Toyofuku, T., and Kitazato, H.: Foraminifera promote calcification by elevating their intracellular pH, P. Natl. Acad. Sci. USA, 106, 15374–15378, https://doi.org/10.1073/pnas.0904306106, 2009.

Durand, M., Mojtahid, M., Maillet, G. M., Baltzer, A., Schmidt, S., Blet, S., Marchès, E., and Howa, H.: Late Holocene record from a Loire River incised paleovalley (French inner continental shelf): Insights into regional and global forcing factors, Palaeogeogr. Palaeocl., 511, 12–28, https://doi.org/10.1016/j.palaeo.2018.06.035, 2018.

Feyling-Hanssen, R. W.: The Foraminifer *Elphidium excavatum* (Terquem) and Its Variant Forms, Micropaleontology, 18, 337–354, https://doi.org/10.2307/1485012, 1972.

Fouet, M.: Répartition des communautés de foraminifères dans les estuaires de la façade atlantique, Thèse de doctorat, Université d'Angers, Université d'Angers, 270 pp., http://www.theses.fr/s227694 (last access: September 2023), 2022.

Fouet, M. P. A., Singer, D., Coynel, A., Héliot, S., Howa, H., Lalande, J., Mouret, A., Schweizer, M., Tcherkez, G., and Jorissen, F. J.: Foraminiferal Distribution in Two Estuarine Intertidal Mudflats of the French Atlantic Coast: Testing the Marine Influence Index, Water, 14, 645, https://doi.org/10.3390/w14040645, 2022.

Geelhoed, J. S., van de Velde, S. J., and Meysman, F. J. R.: Quantification of Cable Bacteria in Marine Sediments via qPCR, Front. Microbiol., 11, 1506, https://doi.org/10.3389/fmicb.2020.01506, 2020.

Geslin, E., Heinz, P., Jorissen, F., and Hemleben, Ch.: Migratory responses of deep-sea benthic foraminifera to variable oxygen conditions: laboratory investigations, Mar. Micropaleontol., 53, 227–243, https://doi.org/10.1016/j.marmicro.2004.05.010, 2004.

Gonzales, M. V., De Almeida, F. K., Costa, K. B., Santarosa, A. C. A., Camillo, E., De Quadros, J. P., and Toledo, F. A. L.: Help Index: Hoeglundina elegans Preservation Index for Marin Sediments in the Western South Atlantic, J. Foramin. Res., 47, 56–69, https://doi.org/10.2113/gsjfr.47.1.56, 2017.

Hansen, H. J.: Shell construction in modern calcareous Foraminifera, in: Modern Foraminifera, Springer Netherlands, Dordrecht, 57–70, https://doi.org/10.1007/0-306-48104-9_4, 1999.

Hansen, H. J. and Lykke-Andersen, A.-L.: Wall structure and classification of fossil and recent Elphidiid and Nonionid Foraminifera, Universitetsforlaget, Oslo, 37 pp., 1976.

Haynert, K., Schönfeld, J., Riebesell, U., and Polovodova, I.: Biometry and dissolution features of the benthic foraminifer Ammonia aomoriensis at high pCO_2, Mar. Ecol. Prog. Ser., 432, 53–67, https://doi.org/10.3354/meps09138, 2011.

Haynert, K., Schönfeld, J., Polovodova-Asteman, I., and Thomsen, J.: The benthic foraminiferal community in a naturally CO_2-rich coastal habitat of the southwestern Baltic Sea, Biogeosciences, 9, 4421–4440, https://doi.org/10.5194/bg-9-4421-2012, 2012.

Haynert, K., Schönfeld, J., Schiebel, R., Wilson, B., and Thomsen, J.: Response of benthic foraminifera to ocean acidification in their natural sediment environment: a long-term culturing experiment, Biogeosciences, 11, 1581–1597, https://doi.org/10.5194/bg-11-1581-2014, 2014.

Haynes, J. R.: Foraminifera, Springer, 475 pp., ISBN: 978-1-349-05399-5, ISBN: 978-1-349-05397-1, 1981.

Hayward, B. W., Holzmann, M., Grenfell, H. R., Pawlowski, J., and Triggs, C. M.: Morphological distinction of molecular types in Ammonia – towards a taxonomic revision of the world's most commonly misidentified foraminifera, Mar. Micropaleontol., 50, 237–271, https://doi.org/10.1016/S0377-8398(03)00074-4, 2004.

Hermans, M., Lenstra, W. K., Hidalgo-Martinez, S., van Helmond, N. A. G. M., Witbaard, R., Meysman, F. J. R., Gonzalez, S., and Slomp, C. P.: Abundance and Biogeochemical Impact of Cable Bacteria in Baltic Sea Sediments, Environ. Sci. Technol., 53, 7494–7503, https://doi.org/10.1021/acs.est.9b01665, 2019.

Hess, S., Alve, E., Trannum, H. C., and Norling, K.: Benthic foraminiferal responses to water-based drill cuttings and natural sediment burial: Results from a mesocosm experiment, Mar. Micropaleontol., 101, 1–9, https://doi.org/10.1016/j.marmicro.2013.03.004, 2013.

Jorissen, F. J., Fouet, M. P. A., Armynot du Châtelet, E., Barras, C., Bouchet, V. M. P., Daviray, M., Francescangeli, F., Geslin, E., Le Moigne, D., Licari, L., Mojtahid, M., Nardelli, M. P., Pavard, J. C., Rolland, A., Schweizer, M., and Singer, D.: Foraminifères estuariens de la façade atlantique française – Guide de détermination, OFB, Université d'Angers, 89 pp., 2023.

Kassambara, A.: Pipe-Friendly Framework for Basic Statistical Tests, R package version 0.7.1, https://CRAN.R-project.org/package=rstatix (last access: April 2023), 2022.

Katz, M. E., Cramer, B. S., Franzese, A., Hönisch, B., Miller, K. G., Rosenthal, Y., and Wright, J. D.: Traditional and emerging geochemical proxies in foraminifera, J. Foramin. Res., 40, 165–192, https://doi.org/10.2113/gsjfr.40.2.165, 2010.

Keul, N., Langer, G., Thoms, S., de Nooijer, L. J., Reichart, G.-J., and Bijma, J.: Exploring foraminiferal Sr/Ca as a new carbonate system proxy, Geochim. Cosmochim. Ac., 202, 374–386, https://doi.org/10.1016/j.gca.2016.11.022, 2017.

Koho, K. A., Piña-Ochoa, E., Geslin, E., and Risgaard-Petersen, N.: Vertical migration, nitrate uptake and denitrification: survival mechanisms of foraminifers (Globobulimina turgida) under low oxygen conditions: Survival mechanisms of foraminifers, FEMS Microbiol. Ecol., 75, 273–283, https://doi.org/10.1111/j.1574-6941.2010.01010.x, 2011.

Kurtarkar, S. R., Nigam, R., Saraswat, R., and Linshy, V. N.: Regeneration and abnormality in benthic foraminifera *Rosalina leei*: Implications in reconstructing past salinity changes, Riv. Ital. Paleontol. Stratigr., 117, 189–196, 2011.

Langlet, D., Geslin, E., Baal, C., Metzger, E., Lejzerowicz, F., Riedel, B., Zuschin, M., Pawlowski, J., Stachowitsch, M., and Jorissen, F. J.: Foraminiferal survival after long-term in situ experimentally induced anoxia, Biogeosciences, 10, 7463–7480, https://doi.org/10.5194/bg-10-7463-2013, 2013.

Langlet, D., Baal, C., Geslin, E., Metzger, E., Zuschin, M., Riedel, B., Risgaard-Petersen, N., Stachowitsch, M., and Jorissen, F. J.: Foraminiferal species responses to *in situ*, experimentally induced anoxia in the Adriatic Sea, Biogeosciences, 11, 1775–1797, https://doi.org/10.5194/bg-11-1775-2014, 2014.

Larsen, S., Nielsen, L. P., and Schramm, A.: Cable bacteria associated with long-distance electron transport in New Eng-

land salt marsh sediment: Cable bacteria in New England salt marsh sediment, Environ. Microbiol. Reports, 7, 175–179, https://doi.org/10.1111/1758-2229.12216, 2015.

Le Cadre, V.: Low pH Effects on Ammonia becarii Test Deformation: Implications for Using Test deformations as a Pollution Indicator, The J. Foramin. Res., 33, 1–9, https://doi.org/10.2113/0330001, 2003.

Lipsewers, Y. A., Vasquez-Cardenas, D., Seitaj, D., Schauer, R., Hidalgo-Martinez, S., Sinninghe Damsté, J. S., Meysman, F. J. R., Villanueva, L., and Boschker, H. T. S.: Impact of Seasonal Hypoxia on Activity and Community Structure of Chemolithoautotrophic Bacteria in a Coastal Sediment, Appl. Environ. Microbiol., 83, e03517-16, https://doi.org/10.1128/AEM.03517-16, 2017.

Malkin, S. Y., Rao, A. M., Seitaj, D., Vasquez-Cardenas, D., Zetsche, E.-M., Hidalgo-Martinez, S., Boschker, H. T., and Meysman, F. J.: Natural occurrence of microbial sulphur oxidation by long-range electron transport in the seafloor, ISME J., 8, 1843–1854, https://doi.org/10.1038/ismej.2014.41, 2014.

Malkin, S. Y., Seitaj, D., Burdorf, L. D. W., Nieuwhof, S., Hidalgo-Martinez, S., Tramper, A., Geeraert, N., De Stigter, H., and Meysman, F. J. R.: Electrogenic Sulfur Oxidation by Cable Bacteria in Bivalve Reef Sediments, Front. Mar. Sci., 4, 19 pp., https://doi.org/10.3389/fmars.2017.00028, 2017.

Malkin, S. Y., Liau, P., Kim, C., Hantsoo, K. G., Gomes, M. L., and Song, B.: Contrasting controls on seasonal and spatial distribution of marine cable bacteria (Candidatus Electrothrix) and Beggiatoaceae in seasonally hypoxic Chesapeake Bay, Limnol. Oceanogr., 67, 1357–1373, https://doi.org/10.1002/lno.12087, 2022.

Martin, R. E.: Environmental Micropaleontology: The Application of Microfossils to Environmental Geology, Kluwer Academic/Plenum Publishers, Springer, 481 pp., https://doi.org/10.1007/978-1-4615-4167-7, 2000.

Marzocchi, U., Trojan, D., Larsen, S., Louise Meyer, R., Peter Revsbech, N., Schramm, A., Peter Nielsen, L., and Risgaard-Petersen, N.: Electric coupling between distant nitrate reduction and sulfide oxidation in marine sediment, ISME J., 8, 1682–1690, https://doi.org/10.1038/ismej.2014.19, 2014.

Marzocchi, U., Bonaglia, S., van de Velde, S., Hall, P. O. J., Schramm, A., Risgaard-Petersen, N., and Meysman, F. J. R.: Transient bottom water oxygenation creates a niche for cable bacteria in long-term anoxic sediments of the Eastern Gotland Basin, Environ.Microbiol., 20, 3031–3041, https://doi.org/10.1111/1462-2920.14349, 2018.

McIntyre-Wressnig, A., Bernhard, J. M., Wit, J. C., and Mccorkle, D. C.: Ocean acidification not likely to affect the survival and fitness of two temperate benthic foraminifera species: results from culture experiements, J. Foramin. Res., 44, 341–351, https://doi.org/10.2113/gsjfr.44.4.341, 2014.

Menier, D. and Dubois, A.: Carte 7137G Natures de fond du Golfe du Morbihan à 1/20000, Service Hydrographique & Océanographique de la Marine, 2011.

Menier, D., Tessier, B., Dubois, A., Goubert, E., and Sedrati, M.: Geomorphological and hydrodynamic forcing of sedimentary bedforms – Example of Gulf of Morbihan (South Brittany, Bay of Biscay), Proceedings of the11th International Coastal Symposium, J. Coast. Res., SI 64, 1530–1534, ISSN 0749-0208, 2011.

Metzger, E., Simonucci, C., Viollier, E., Sarazin, G., Prévot, F., and Jézéquel, D.: Benthic response to shellfish farming in Thau lagoon: Pore water signature, Estuar. Coast. Shelf Sci., 72, 406–419, https://doi.org/10.1016/j.ecss.2006.11.011, 2007.

Meysman, F. J. R., Risgaard-Petersen, N., Malkin, S. Y., and Nielsen, L. P.: The geochemical fingerprint of microbial long-distance electron transport in the seafloor, Geochim. Cosmochim. Ac., 152, 122–142, https://doi.org/10.1016/j.gca.2014.12.014, 2015.

Michaud, E., Aller, R., Zhu, Q., Heilbrun, C., and Stora, G.: Density and size-dependent bioturbation effects of the infaunal polychaete *Nephtys incisa* on sediment biogeochemistry and solute exchange, J. Mar. Res., 79, 181, https://doi.org/10.1357/002224021834670801, 2021.

Middelburg, J. J., Soetaert, K., and Hagens, M.: Ocean Alkalinity, Buffering and Biogeochemical Processes, Rev. Geophys., 58, e2019RG000681, https://doi.org/10.1029/2019RG000681, 2020.

Mojtahid, M., Depuydt, P., Mouret, A., Le Houedec, S., Fiorini, S., Chollet, S., Massol, F., Dohou, F., Filipsson, H. L., Boer, W., Reichart, G.-J., and Barras, C.: Assessing the impact of different carbonate system parameters on benthic foraminifera from controlled growth experiments, Chem. Geol., 623, 121396, https://doi.org/10.1016/j.chemgeo.2023.121396, 2023.

Murray, J. W.: British Nearshore Foraminiferids, Academic Press, London, 68 pp., ISBN: 012-511850-3, 1979.

Murray, J. W.: Ecology and Applications of Benthic Foraminifera, Cambridge University Press, 320 pp., ISBN: 978-0-521-82839-0, 2006.

Nielsen, L. P., Risgaard-Petersen, N., Fossing, H., Christensen, P. B., and Sayama, M.: Electric currents couple spatially separated biogeochemical processes in marine sediment, Nature, 463, 1071–1074, https://doi.org/10.1038/nature08790, 2010.

Office Français De La Biodiversité Découvrir Les Estuaires de La Façade Manche/Atlantique – Le Portail Technique De l'OFB, https://professionnels.ofb.fr/fr/node/276, last access: 29 Novembre 2023.

Patterson, R. T. and Fishbein, E.: Re-examination of the statistical methods used to determine the number of point counts needed for micropaleontological quantitative research, J. Paleontol., 63, 245–248, https://doi.org/10.1017/S0022336000019272, 1989.

Petersen, J., Barras, C., Bézos, A., La, C., de Nooijer, L. J., Meysman, F. J. R., Mouret, A., Slomp, C. P., and Jorissen, F. J.: Mn/Ca intra- and inter-test variability in the benthic foraminifer *Ammonia tepida*, Biogeosciences, 15, 331–348, https://doi.org/10.5194/bg-15-331-2018, 2018.

Pfeffer, C., Larsen, S., Song, J., Dong, M., Besenbacher, F., Meyer, R. L., Kjeldsen, K. U., Schreiber, L., Gorby, Y. A., El-Naggar, M. Y., Leung, K. M., Schramm, A., Risgaard-Petersen, N., and Nielsen, L. P.: Filamentous bacteria transport electrons over centimetre distances, Nature, 491, 218–221, https://doi.org/10.1038/nature11586, 2012.

Polovodova, I. and Schonfeld, J.: Foraminiferal Test Abnormalities in the Western Baltic Sea, J. Foramin. Res., 38, 318–336, https://doi.org/10.2113/gsjfr.38.4.318, 2008.

Pucci, F., Geslin, E., Barras, C., Morigi, C., Sabbatini, A., Negri, A., and Jorissen, F. J.: Survival of benthic foraminifera under hypoxic conditions: Results of an experimental study using

the CellTracker Green method, Mar. Pollut. Bull., 59, 336–351, https://doi.org/10.1016/j.marpolbul.2009.08.015, 2009.

R Core Team: R: A language and environment for statistical computing. R Foundation for Statistical Computing, Vienna, Austria, https://www.R-project.org/ (last access: April 2023), 2022.

Rao, A. M. F., Malkin, S. Y., Hidalgo-Martinez, S., and Meysman, F. J. R.: The impact of electrogenic sulfide oxidation on elemental cycling and solute fluxes in coastal sediment, Geochim. Cosmochim. Ac., 172, 265–286, https://doi.org/10.1016/j.gca.2015.09.014, 2016.

Réseau: SYVEL Système de veille dans l'estuaire de la Loire GIP Loire Estuaire, https://www.loire-estuaire.org/dif/do/init, last assess: 29 Novembre 2023.

Revsbech, N. P.: An oxygen microsensor with a guard cathode, Limnol. Oceanogr., 34, 474–478, https://doi.org/10.4319/lo.1989.34.2.0474, 1989.

Revsbech, N. P. and Jørgensen, B. B.: Microelectrodes: Their Use in Microbial Ecology, in: Advances in Microbial Ecology, Vol. 9, edited by: Marshall, K. C., Springer US, Boston, MA, 293–352, https://doi.org/10.1007/978-1-4757-0611-6_7, 1986.

Richirt, J., Schweizer, M., Bouchet, V. M. P., Mouret, A., Quinchard, S., and Jorissen, F. J.: Morphological Distinction of Three Ammonia Phylotypes Occurring Along European Coasts, J. Foramin. Res., 49, 76–93, https://doi.org/10.2113/gsjfr.49.1.76, 2019.

Richirt, J., Guihéneuf, A., Mouret, A., Schweizer, M., Slomp, C. P., and Jorissen, F. J.: A historical record of benthic foraminifera in seasonally anoxic Lake Grevelingen, the Netherlands, Palaeogeogr. Palaeocl., 599, 111057, https://doi.org/10.1016/j.palaeo.2022.111057, 2022.

Risgaard-Petersen, N., Revil, A., Meister, P., and Nielsen, L. P.: Sulfur, iron-, and calcium cycling associated with natural electric currents running through marine sediment, Geochim. Cosmochim. Ac., 92, 1–13, https://doi.org/10.1016/j.gca.2012.05.036, 2012.

Risgaard-Petersen, N., Damgaard, L. R., Revil, A., and Nielsen, L. P.: Mapping electron sources and sinks in a marine biogeobattery, J. Geophys. Res.-Biogeo., 119, 1475–1486, https://doi.org/10.1002/2014JG002673, 2014.

Risgaard-Petersen, N., Kristiansen, M., Frederiksen, R. B., Dittmer, A. L., Bjerg, J. T., Trojan, D., Schreiber, L., Damgaard, L. R., Schramm, A., and Nielsen, L. P.: Cable Bacteria in Freshwater Sediments, Appl. Environ. Microbiol., 81, 6003–6011, https://doi.org/10.1128/AEM.01064-15, 2015.

Scholz, V. V., Martin, B. C., Meyer, R., Schramm, A., Fraser, M. W., Nielsen, L. P., Kendrick, G. A., Risgaard-Petersen, N., Burdorf, L. D. W., and Marshall, I. P. G.: Cable bacteria at oxygen-releasing roots of aquatic plants: a widespread and diverse plant–microbe association, New Phytol., 232, 2138–2151, https://doi.org/10.1111/nph.17415, 2021.

Schönfeld, J. and Mendes, I.: Benthic foraminifera and pore water carbonate chemistry on a tidal flat and salt marsh at Ria Formosa, Algarve, Portugal, Estuar. Coast. Shelf Sci., 276, 108003, https://doi.org/10.1016/j.ecss.2022.108003, 2022.

Scott, D. B., Schafer, C. T., and Medioli, F. S.: Eastern Canadian estuarine foraminifera; a framework for comparison, J. Foramin. Res., 10, 205–234, https://doi.org/10.2113/gsjfr.10.3.205, 1980.

Seitaj, D., Schauer, R., Sulu-Gambari, F., Hidalgo-Martinez, S., Malkin, S. Y., Burdorf, L. D. W., Slomp, C. P., and Meysman, F. J. R.: Cable bacteria generate a firewall against euxinia in seasonally hypoxic basins, P. Natl. Acad. Sci. USA, 112, 13278–13283, https://doi.org/10.1073/pnas.1510152112, 2015.

Soetaert, K., Hofmann, A. F., Middelburg, J. J., Meysman, F. J. R., and Greenwood, J.: The effect of biogeochemical processes on pH, Mar. Chem., 105, 30–51, https://doi.org/10.1016/j.marchem.2006.12.012, 2007.

Thibault de Chanvalon, A., Metzger, E., Mouret, A., Cesbron, F., Knoery, J., Rozuel, E., Launeau, P., Nardelli, M. P., Jorissen, F. J., and Geslin, E.: Two-dimensional distribution of living benthic foraminifera in anoxic sediment layers of an estuarine mudflat (Loire estuary, France), Biogeosciences, 12, 6219–6234, https://doi.org/10.5194/bg-12-6219-2015, 2015.

Thibault de Chanvalon, A., Mouret, A., Knoery, J., Geslin, E., Péron, O., and Metzger, E.: Manganese, iron and phosphorus cycling in an estuarine mudflat, Loire, France, J. Sea Res., 118, 92–102, https://doi.org/10.1016/j.seares.2016.10.004, 2016a.

Thibault de Chanvalon, A., Metzger, E., Mouret, A., Knoery, J., Chiffoleau, J.-F., and Brach-Papa, C.: Particles transformation in estuaries: Fe, Mn and REE signatures through the Loire Estuary, J. Sea Res., 118, 103–112, https://doi.org/10.1016/j.seares.2016.11.004, 2016b.

Thibault de Chanvalon, A., Metzger, E., Mouret, A., Knoery, J., Geslin, E., and Meysman, F. J. R.: Two dimensional mapping of iron release in marine sediments at submillimetre scale, Mar. Chem., 191, 34–49, https://doi.org/10.1016/j.marchem.2016.04.003, 2017.

Thibault de Chanvalon, A., Geslin, E., Mojtahid, M., Métais, I., Méléder, V., and Metzger, E.: Multiscale analysis of living benthic foraminiferal heterogeneity: Ecological advances from an intertidal mudflat (Loire estuary, France), Cont. Shelf Res., 232, 104627, https://doi.org/10.1016/j.csr.2021.104627, 2022.

Toyofuku, T., Matsuo, M. Y., de Nooijer, L. J., Nagai, Y., Kawada, S., Fujita, K., Reichart, G.-J., Nomaki, H., Tsuchiya, M., Sakaguchi, H., and Kitazato, H.: Proton pumping accompanies calcification in foraminifera, Nat. Commun., 8, 14145, https://doi.org/10.1038/ncomms14145, 2017.

van Cappellen, P. and Wang, Y.: Cycling of iron and manganese in surface sediments: A general theory for the coupled transport and reaction of carbon, oxygen, nitrogen, sulfur, iron, and manganese, Am. J. Sci., 296, 197–243, 1996.

van de Velde, S., Lesven, L., Burdorf, L. D. W., Hidalgo-Martinez, S., Geelhoed, J. S., Van Rijswijk, P., Gao, Y., and Meysman, F. J. R.: The impact of electrogenic sulfur oxidation on the biogeochemistry of coastal sediments: A field study, Geochim. Cosmochim. Ac., 194, 211–232, https://doi.org/10.1016/j.gca.2016.08.038, 2016.

World Register of Marine Species (WoRMS): https://www.marinespecies.org/index.php, last assess: 5 May 2022.